Photogeneration of Charge Carriers and Their Transport Properties in Poly[bis(*p*-*n*-butylphenyl)silane]

Anjali Acharya, Shu Seki,* Yoshiko Koizumi, Akinori Saeki, and Seiichi Tagawa*

The Institute of Scientific and Industrial Research, Osaka University, 8-1 Mihogaoka, Ibaraki, Osaka 567-0047, Japan

Received: June 20, 2005; In Final Form: September 8, 2005

The photocarrier generation mechanism and mobility in poly[bis(*p*-*n*-butylphenyl)silane] (PBPS) thin films doped with a variety of electron acceptors are studied by time-resolved microwave conductivity (TRMC) measurements. It was found that fullerene is a suitable electron acceptor for PBPS as it provides the highest product of photocarrier generation yield ϕ and mobility $\Sigma\mu$ under excitation at 532 and 355 nm. The observed high $\phi\Sigma\mu$ value of 4.5×10^{-3} cm^2/(V s) under excitation at 193 nm (6.39 eV) can be attributed to the direct ionization of PBPS molecules. The photoinduced electron transfer between C_{60} and PBPS was investigated in a solution sample by laser flash photolysis under excitation at 532 nm. On the basis of the extinction coefficient of PBPS$^{\bullet+}$, transient absorption of PBPS$^{\bullet+}$ provides a maximum value of ϕ of 0.83% for the electron-transfer reaction from PBPS to $^3C_{60}$*. On the basis of this value of ϕ, the intrinsic intrachain mobility of holes on the PBPS backbone is estimated to be higher than 1.7×10^{-2} cm^2/(V s), suggesting the presence of a high conducting path along the Si backbone of PBPS.

Introduction

Recent observations of high-efficiency room-temperature electroluminescence (EL) from the diarylpolysilane poly[bis(*p*-*n*-butylphenyl)silane] (PBPS) have attracted much attention in both fundamental and applied research. A method has been successfully developed for the fabrication of PBPS-based light-emitting diodes (LEDs) that exhibit efficient near-ultraviolet electroluminescence (NUV EL) at room temperature.[1−5] There have been several EL studies on polysilanes with diverse substituents.[6−12] However, weak UV and NUV EL from polysilanes at low temperature have limited their applications as emissive materials for LEDs. Recently, Hoshino et al.[4] succeeded in observing improved EL performance in a double-layer LED with a 2-(4′-*tert*-butylphenyl)-5-(4″-biphenyl)-1,3,4-oxadiazole-based electron transport layer, observing an EL external quantum efficiency twice that of a PBPS single-layer LED. The relatively small band gap and higher thermal/chemical stability of PBPS compared to poly(methylphenylsilane) (PMPS) or dialkylpolysilane are responsible for the exceptional performance of PBPS LEDs. On the basis of ab initio calculations, Sharma et al.[13] proved the possibility of stabilizing PBPS and PMPS by intersystem crossing from the S_1 state to the T_1 excited state, which in turn leads to a higher stability of these two polymers. PBPS exhibits a thermal phase transition accompanied by conformational changes in the polymer backbone, from a disordered form (low-temperature phase) to a trans-planar form (high-temperature phase).[14] This structural phase transition at 350−360 K has a beneficial effect on the EL characteristics of PBPS LEDs. Polysilanes exhibit efficient photoluminescence with a relatively small spectral bandwidth in the UV or NUV region.[15]

Diarylpolysilanes with tightly locked Si backbones are candidates for ideal one-dimensional (1-D) structures that would show 1-D semiconductor and/or quantum wire properties.[16] The author has reported transient spectroscopy of ion radicals and dynamics of charge carriers on poly[bis(*p*-alkylphenyl)silane] compounds using electron beam pulse radiolysis. Hoshino et al.[17] investigated the molecular weight dependence of the carrier transport properties of PBPS thin films by using the time-of-flight (TOF) technique. PBPS has a particular carrier transport property: not only does it have the hole transport property generally found in polysilanes but it also exhibits an electron transport property.[17,18] On the basis of the above reports, it has been revealed that PBPS is a potential candidate for many optoelectronic applications. However, for this novel polymer to be used in these optoelectronic applications, the charge carrier generation and mobility must be optimized. For example, conjugated polymer thin film transistors (TFTs) in logic circuits or pixel switching elements in displays[19] require high charge carrier mobilities exceeding 0.1 cm^2/(V s).[20]

The electrodeless flash-photolysis time-resolved microwave conductivity (FP-TRMC)[21−27] technique is a unique tool for measuring the intrinsic dynamics of charge carriers in photosensitized materials and conjugated polymers. With this technique, it is possible to monitor changes in conductivity during pulsed laser excitation on a nanosecond time scale, without contacting the sample with electrodes. A change in the conductivity of a medium resulting from mobile charge carriers is measured as a change in the power level of the microwaves. The efficiency of the photogeneration of charge carriers in polymers increases upon the addition of acceptor molecules with increasing electron affinity,[28−31] which can be attributed to the formation of charge transfer (CT) complexes in the polymer.

In this paper, we report on the choice of suitable electron acceptor for PBPS to optimize the photocarrier generation yield. The generation mechanism of photocarriers and their transport in PBPS film samples were investigated using FP-TRMC with

* To whom correspondence should be addressed. E-mail: seki@bms.sanken.osaka-u.ac.jp. Tel: +81-6-6879-8502. Fax: +81-6-6876-3287 (S. Seki). E-mail: tagawa@sanken.osaka-u.ac.jp. Tel: +81-6-6879-8500. Fax: +81-6-6876-3287 (S. Tagawa).

10.1021/jp053300h CCC: $30.25
Published on Web 10/12/2005

a variety of excitation light sources. We also investigated the electron-transfer process between electron acceptors and PBPS in solution by laser flash photolysis.

Experimental Section

General. Reagents and chemicals were purchased from Wako Chemical Co. or Aldrich Chemical Co. unless otherwise stated. As electron acceptors, we used fullerene (C_{60} from MTR Ltd.), 1,2,4,5-tetracyanobenzene (TCNB), 1,4-dinitrobenzene (DNB), tetracynoquinodimethane (TCNQ), bromanil, and chloranil. Film samples were prepared by a drop-cast method onto a quartz substrate and dried in a vacuum oven at 55 °C for 2−3 h using PBPS (68 mmol dm^{-3}, base mol unit)/dopant (5 mmol dm^{-3}) mixture solutions in toluene or *o*-dichlorobenzene. The thicknesses of the films were 5−8 μm, measured using a Dektak^3-ST surface profiler. The absorbance of the film samples was measured using a Shimadzu UV-3100PC spectrophotometer.

Synthesis. Bis(*p*-*n*-butylphenyl)-dichlorosilane, the monomer of PBPS, was synthesized by a stepwise condensation of *p*-*n*-butylphenylmagnesiumbromide with tetrachlorosilane or trichlorosilane.[16,32,33] Solutions of *p*-*n*-butylphenylmagnesiumbromide in diethyl ether were obtained by reacting 4-*n*-butylphenylbromide with magnesium metal. Tetrachlorosilane (1.2 equiv) was then added to the solution and stirred for 12 h. The solutions were refluxed for another 2 h. After filtration, the solution was concentrated and distilled, giving *p*-*n*-butylphenyltrichlorosilane (bp 90 °C at 2 Torr). Condensation of the trichlorosilane with the same Grignard reagent was carried out in a similar manner. The obtained bis(*p*-*n*-butylphenyl)-dichlorosilane was distilled at least three times prior to use (yield, 80%). *N*-hexylphenyl-dichlorosilane, the monomer of poly(*n*-hexylphenylsilane) (PHPS), was prepared in a similar manner as described elsewhere.[33] The monomer of PMPS was purchased from Shin-Etsu Chemical Co. Ltd. and distilled twice prior to use. Polymerization was carried out by the Kipping method using the dichlorosilane with sodium metal in dry toluene for 5−20 h at 110 °C.[34,35] The polymer solution was precipitated in isopropyl alcohol (IPA) after filtration through a 0.45-mm PTFE filter to eliminate NaCl, and the precipitates were dried in a vacuum (yield, 12−18%). The toluene solutions of the polymers were transferred to a separating funnel, washed with water to eliminate remaining NaCl, and precipitated twice with toluene−IPA and THF−methanol. The molecular weights (M_n) of the PMPS, PHPS, and PBPS were 4.8×10^4, 1.1×10^6, and 9.0×10^3, respectively, with a small dispersion ($M_w/M_n < 2.2$), determined by gel permeation chromatography based on polystyrene standards.

Bis(*p*-*n*-butylphenyl)-dichlorosilane. Bp 193−195 °C at 0.5 Torr. ^{1}H NMR (270 MHz, $CDCl_3$), δ 0.92 (t, 3H, CH_3), 1.27−1.43 (m, 8H, CH_2), 1.51−1.67 (m, 8H, CH_2), 7.24−7.27 (d, 2H, ArH), 7.63−7.66 (d, 2H, ArH).

Flash Photolysis. Nanosecond laser pulses from an excimer laser (ArF (193 nm), Lambda Physics, Compex 102, fwhm 5−8 ns) and Nd:YAG lasers (third harmonic generation (355 nm) and second harmonic generation (532 nm) from Spectra Physics, GCR-130, fwhm 5−8 nm) were used as excitation sources. Transient conductivity and optical absorption were measured with an identical geometry using TRMC and TOS (time-resolved optical spectroscopy) systems. The photon density of the laser was set at 3.7×10^{16} photons/cm^2 for TRMC and 2.2×10^{17} photons/cm^2 for TOS. A white light continuum from a Xe lamp was used as a probe light source. The probe light and the emission were guided into a high-dynamic-range streak camera (Hamamatsu C7700) that collects 2-D images of light intensity spectra. TOS was performed on a deaerated solution obtained by Ar bubbling in a square quartz cell at room temperature.

TABLE 1: Values of $\phi\Sigma\mu$ in PBPS Films Doped with Various Dopants under Excitation at 532 and 355 nm

dopant[a]	$\phi\Sigma\mu$ ($\times 10^{-5}$ cm^2/(V s)) at 532 nm excitation	$\phi\Sigma\mu$ ($\times 10^{-5}$ cm^2/(V s)) at 355 nm excitation
fullerene (C_{60})	36	9.2
TCNB[b]	12	2.7
DNB[c]	13	1.4
TCNQ[d]	1.2	2.5
bromanil	1.4	1.3
chloranil	7.4	2.3

[a] Concentration of the dopants at 7.4 mol % relative to the number of Si repeating units in PBPS. [b] 1,2,4,5-Tetracyanobenzene. [c] 1,4-Dinitrobenzene. [d] Tetracyanoquinodimethane.

For TRMC, the microwave frequency and power were set at ~9.1 GHz and 3 mW, respectively, so that the motion of the charge carriers would not be disturbed by the low electric field of the microwaves. The TRMC signal, picked up by a diode (rise time < 1ns), was monitored by a digital oscilloscope (Tektronix, TDS3052B, rise time 0.7 ns).

All the above experiments were carried out at room temperature.

The transient photoconductivity ($\Delta\sigma$) of a polymer film is related to the reflected microwave power ($\Delta P_r/P_r$) and the sum of the mobilities of the charge carriers via

$$\langle \Delta\sigma \rangle = \frac{1}{A}\frac{\Delta P_r}{P_r} \tag{1}$$

$$\Delta\sigma = N \times e \sum \mu\phi \tag{2}$$

where A, N, e, ϕ, and $\Sigma\mu$ are the sensitivity factor, the number of absorbed photons per unit volume, elementary charge of an electron, photocarrier generation yield (quantum efficiency), and sum of mobilities for negative and positive carriers, respectively. The number of photons absorbed by a sample was estimated based on the steady-state absorption spectrum, taken into account as the sensitivity factor A.

Further details on the experimental apparatus are described elsewhere.[27]

Results and Discussion

The quantum efficiency of photogeneration of charge carriers and their mobility are important factors that determine the photoconductive properties of polymers. The enhancement of photoconductive properties in conjugated polymer films[26,36,37] due to dopants can be attributed to the photoinduced electron transfer between dopants and the polymer. The effects of various dopants on the value of $\phi\Sigma\mu$ observed by FP-TRMC measurements are summarized in Table 1. The electron acceptor fullerene (C_{60}) (Figure 1) was found to be the most suitable for PBPS as it gives higher $\phi\Sigma\mu$ values (excitation at 532 nm, 36×10^{-5} cm^2/(V s); at 355 nm, 9.2×10^{-5} cm^2/(V s)). In the steady-state absorption spectra of doped film samples, a broad absorption band (450−550 nm) has been observed for the C_{60}-doped film sample. The effective photoinduced electron transfer between the polymer and C_{60} might cause an increase in the $\phi\Sigma\mu$ value.

Figure 2 shows the conductivity transients observed for a variety of polysilane derivatives with the same concentration of C_{60} as an additive. The estimated $\phi\Sigma\mu$ values are 1 order of magnitude higher in PHPS and PBPS than in PMPS. The backbone conformation of Si chains in PBPS and PHPS has

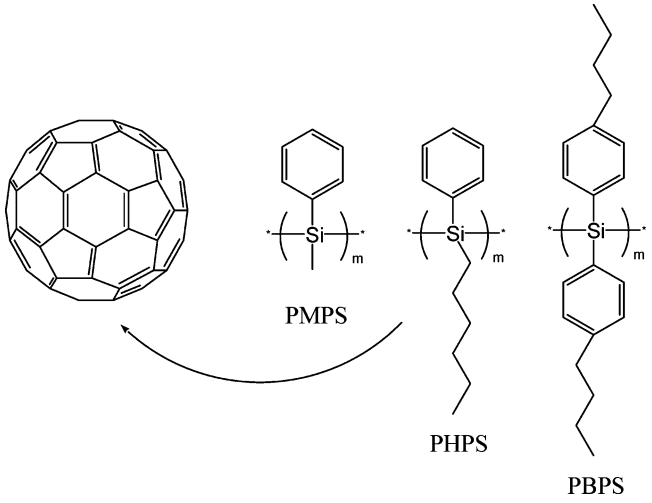

Figure 1. Chemical structures of polysilane derivatives and C_{60}.

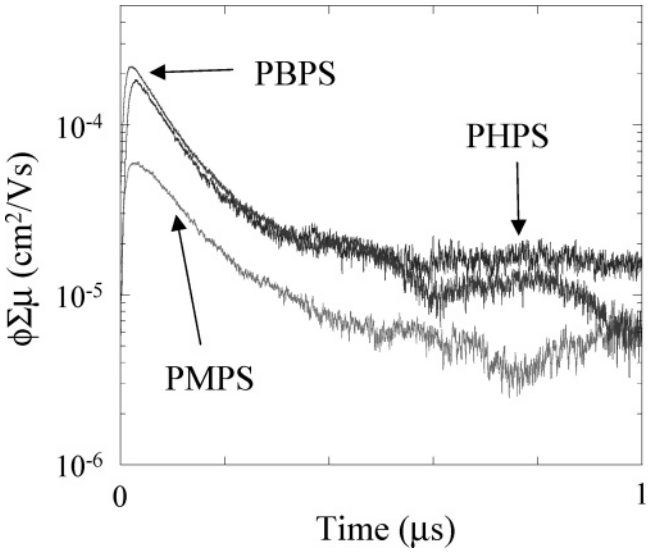

Figure 2. Conductivity transients for C_{60}-doped PMPS, PHPS, and PBPS films at 2.8 mol % concentrated recorded under an excitation at 532 nm.

been found to have a stiff, rodlike structure with a longer persistence length of 4.5−10 nm than that in the wormlike Si chains of PMPS, with a persistence length of 1.1 nm.[16,33] PBPS and PHPS have also been reported to show a higher degree of delocalization of charge carriers over a few tens of Si repeating units than that in PMPS.[33] This explains the higher values of $\phi\Sigma\mu$, especially in PBPS.

It is important to optimize the concentration of fullerenes in a PBPS sample. Figure 3 shows the dependence of the mobility of charge carriers on fullerene concentration in PBPS film samples upon exposure to 532-nm laser pulses. The mobility increases linearly with an increase in fullerene concentration of 0−10 mol % and seems to saturate at higher concentrations. Because of the solubility of C_{60}, quantitative values of $\phi\Sigma\mu$ at concentrations of C_{60} higher than 30% could not be obtained, as such concentrations apparently induced nonhomogeneity in the films.

The increase in $\phi\Sigma\mu$ with increased concentration is attributed mainly to the following factors: (1) changes in the dipole moment of the film, (2) an increase in ϕ due to aggregation of C_{60}, and (3) a contribution from μ_- of the electrons of C_{60} and/or C_{60} aggregates. For the first factor, the hole drift mobility is influenced by the dipole moment of the dopants in the

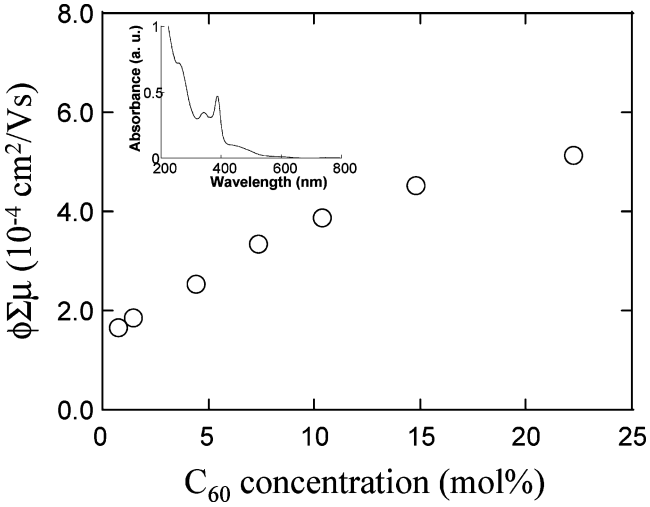

Figure 3. Dependence of $\phi\Sigma\mu$ on C_{60} concentration (mol %) in PBPS films under excitation at 532 nm. The inset figure shows the absorption spectrum of the C_{60}-doped PBPS film sample at 12 mol %.

molecularly doped system.[31] Many researchers have reported electron transfer between fullerene and polymers.[30,36,37] The decrease in the total dielectric constant induced by doping with C_{60} (with a low dipole moment) often causes an increase in the mobility but reduces ϕ. For the second factor, the absorption spectrum of a PBPS film doped with C_{60} is displayed in the inset of Figure 3. A small shift in the absorption peak attributed to C_{60} at ∼500 nm suggests that C_{60} molecules distribute homogeneously in the film at low concentration with a small contribution from C_{60} aggregates. However, the contribution of aggregates is significant at higher concentrations of C_{60}, giving a featureless broad absorption. This is related to the third factor. The $\phi\Sigma\mu$ value in Figure 3 is the product of ϕ and $\Sigma\mu = \mu_+ + \mu_-$, that is, the sum of the mobility of positive and negative charge carriers. It has been reported that negative charge carriers trapped at C_{60} ($C_{60}^{\bullet-}$) or at aggregates contribute significantly to conductivity transients. A drastic increase in $\phi\Sigma\mu$ is typically observed in films containing extremely high concentrations of C_{60}, over 60 wt %.[38] Thus, considering these factors, the conductivity transients observed at lower concentrations of C_{60} reflect predominantly the intrinsic mobility of positive charge carriers on the polymer backbone. The saturation of $\phi\Sigma\mu$ at higher fullerene concentrations (>15 mol %) may be due to exciton−exciton annihilation reactions (specifically, the triplet−triplet annihilation reaction), which predominate over the charge-transfer reaction between PBPS and $^3C_{60}$*. To eliminate the contribution of the above factors and to estimate the intrinsic value of $\phi\Sigma\mu$ without the contribution from the dopants, extrapolation of Figure 3 gives a $\phi\Sigma\mu$ value in PBPS of 1.4×10^{-4} cm^2/(V s) at the zero limit of C_{60} concentration.

The ArF (193 nm → 6.39 eV) and YAG (532 nm → 2.32 eV) lasers have different photon energies and were used to excite film samples, as shown in Figure 4. By the use of the ArF laser, charge carriers were generated directly in the film samples as the photon energy is greater than the band energy (>3.5 eV) and ionization potential (<6 eV) of PBPS. Almost identical conductivity traces were observed for both PBPS and C_{60}-doped PBPS films under an excitation at 193 nm, suggesting that C_{60} does not contribute in the case of high photon energy (6.39 eV). The observed $\phi\Sigma\mu$ value (4.52×10^{-3} cm^2/(V s)) is much higher than that observed for PMPS (1.22×10^{-3} cm^2/(V s)) using the same TRMC technique.[39] In Figure 4b, we can clearly distinguish the differences in the initial decay kinetics of charge carriers generated under excitations at 193 and 532 nm. The

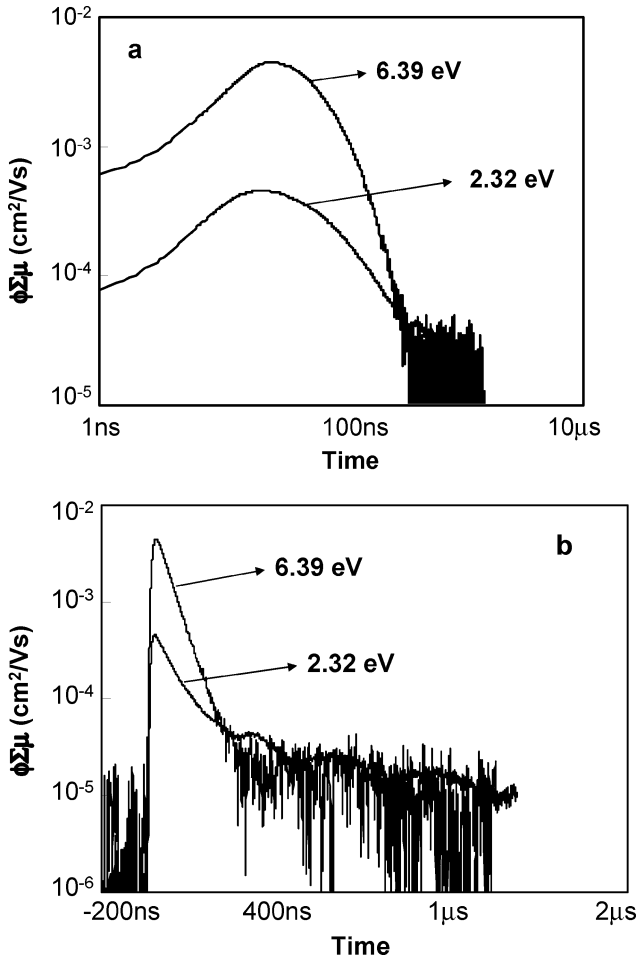

Figure 4. Conductivity transients for C_{60}-doped PBPS films on (a) logarithmic and (b) linear time scales under an excitation at two different photon energies: 193 nm (6.39 eV) and 532 nm (2.32 eV).

initial fast decay under an excitation at 193 nm is due to a combination of $PBPS^{\bullet+}$ and e^-, with a rate constant of 1.7×10^7 s^{-1}, whereas for the 532-nm excitation, the backward electron transfer between $PBPS^{\bullet+}$ and $C_{60}^{\bullet-}$ causes a fast initial decay with a rate constant of 6.5×10^6 s^{-1}. The slow decay in both cases can be attributed to charge recombination after diffusion.[27]

Bleyl et al.[14] have observed the existence of a structural transformation at around 354 K for PBPS that accompanies a conformational change of the backbone. PBPS molecules tend to be in a disordered conformation at room temperature, whereas they are in an ordered configuration at temperatures higher than about 360 K. The transformation of the backbone was reflected as a thermochromic shift of the NUV absorption of polysilanes; PBPS showed a gradual red shift of the band with increasing temperature. This type of thermochromic behavior has often been observed for diaryl-substituted polysilanes, in striking contrast to dialkyl-substituted polysilanes that show a clear blue shift with an isosbestic point. TRMC traces of PBPS at room temperature and 360 K are shown in Figure 5. The two traces appear to overlap, indicating that there is no considerable enhancement of the charge carrier mobility at the higher temperature. A drastic mobility enhancement at the disorder−order transition has often been observed in dialkyl-substituted polysilanes, not only by TRMC[40] but also by conventional time-of-flight (TOF) techniques.[41] However, the present results suggest that the transition of PBPS is not a pronounced

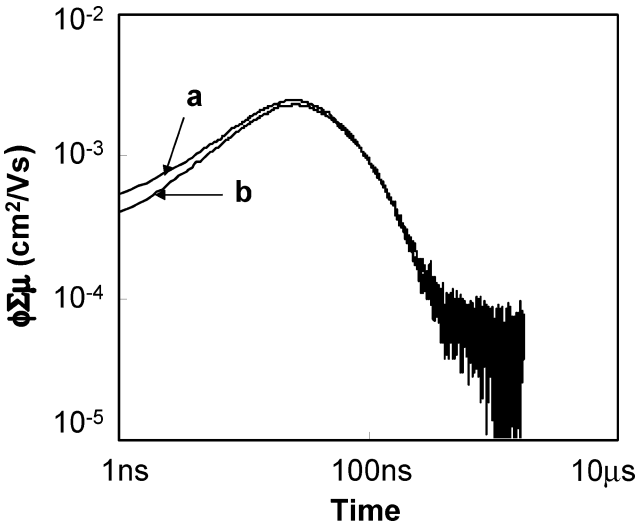

Figure 5. Conductivity transients for a C_{60}-doped PBPS film sample (a) at room temperature and (b) at 360 K.

transformation causing a remarkable elongation of the backbone conjugated system.

To determine the photocarrier generation yield ϕ, TOS observations were performed for PBPS−C_{60} systems. A transient absorption spectrum of a PBPS−C_{60} solution in *o*-dichlorobenzene/benzonitrile (DCB/BN = 1:1) is shown in Figure 6 together with the kinetic traces monitored at the corresponding absorption bands. Under excitation at 532 nm, two transient absorption bands appear clearly at 406 and 740 nm. These absorption maxima can be attributed to $PBPS^{\bullet+}$ and $^3C_{60}$*, respectively.[16,35] The absorption maximum of $C_{60}^{\bullet-}$, which shows a transient absorption at the near-IR region, was not detectable with the present apparatus. The following expression of form is suggested as a scheme of the direct electron transfer from PBPS to $^3C_{60}$* in a DCB/BN mixed solvent

$$^3C_{60}^* + \text{PBPS} \xrightarrow{k_{et}} C_{60}^{\bullet-} + \text{PBPS}^{\bullet+} \tag{3}$$

For a photon energy of 2.32 eV (532 nm), C_{60} molecules are first excited to the singlet state and then transferred to the triplet state within a few nanoseconds with an extremely high intersystem crossing ratio (∼1).[37] This photon energy would not excite a PBPS molecule directly. A kinetic trace of the formation of $PBPS^{\bullet+}$ is also shown in the inset of Figure 6c. On the basis of the rise time, the formation rate constant of $PBPS^{\bullet+}$ was calculated as $\sim 2 \times 10^9$ mol^{-1} dm^3 s^{-1}, which is 1 order of magnitude higher than the rate constant of PMPS radical cations, reported as 2×10^8 mol^{-1} dm^3 s^{-1}.[37,42,43] One factor accelerating the electron-transfer reaction in the present case may be the lower molecular weight of PBPS. The formation process was fast enough in comparison with the decay rate of $^3C_{60}$*;[46] the maximum transient absorbance ΔA at 406 nm was determined to be $\Delta A = 0.23$ cm^{-1}. Radical cations of PBPS ($PBPS^{\bullet+}$) showed a strong transient absorption band at 406 nm, and the extinction coefficient ϵ^+ of the band at 406 nm was reported to be 2.0×10^5 M^{-1} cm^{-1}.[16,33,44,45] The concentration of generated $PBPS^{\bullet+}$ in the solution sample can be estimated as

$$[\text{PBPS}^{\bullet+}] = \frac{\Delta A}{\epsilon^{\bullet+}} \tag{4}$$

By combining the value of ΔA and ϵ^+ in the above equation, $[PBPS^{\bullet+}]$ is estimated to be 1.1×10^{-6} M^{-1}, giving a quantum

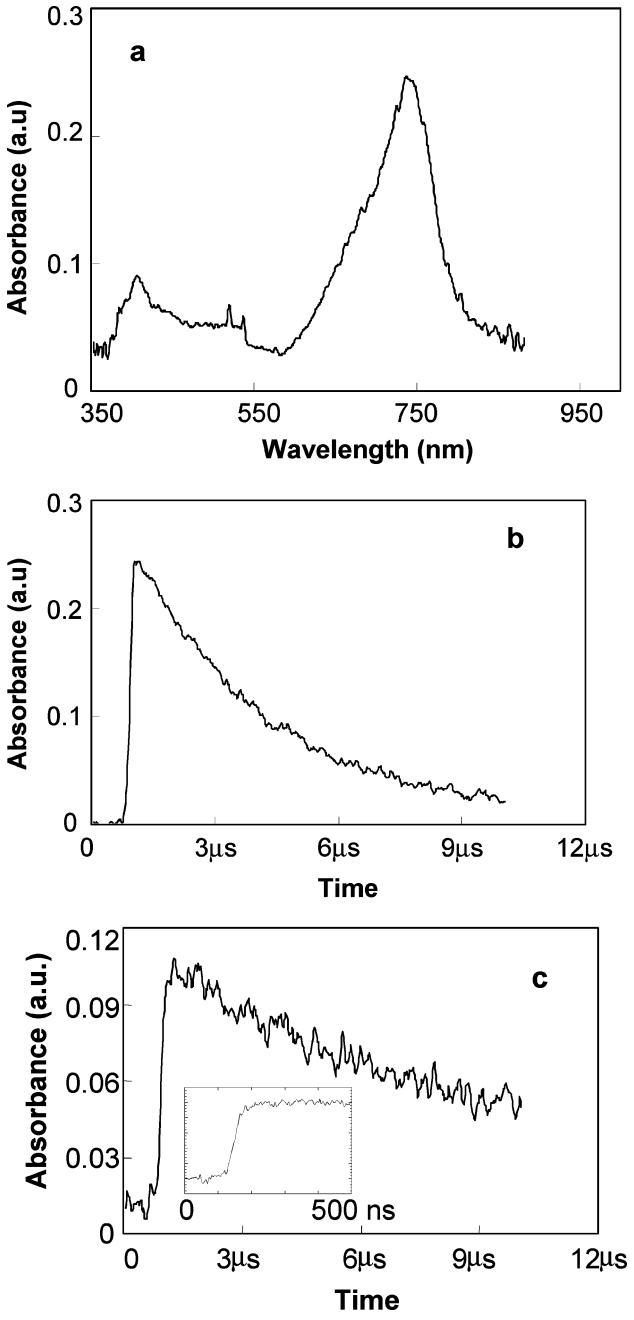

Figure 6. Transient absorption spectrum and kinetics obtained by laser flash photolysis of 5-mM PBPS (base mol unit) in the presence of 1-mM C_{60} in DCB/BN = 1:1 mixed solvent under excitation at 532 nm: (a) absorption spectrum observed at 100 ns after pulse exposure, (b) decay kinetics at 745−765 nm, and (c) decay kinetics at 405−425 nm. The inset in graph c shows the kinetic trace over a shorter time region.

efficiency of reaction 3 as $\phi = 0.83\%$, based on an absorbed photon density of 7.9×10^{16} cm^{-3}. The value of ϕ decreased with an increase in the amount of *o*-dichlorobenzene in the mixture solvent and hence with a decrease in the polarity of the solvent. This suggests that ϕ is lower in the solid state mixture of PBPS and C_{60} in which the dipole moment of the Si repeating unit in PBPS is considerably lower than that of benzonitrile. No significant transient absorption at ∼406 nm was observed for the film samples even for an exposure to a photon density 1 order of magnitude higher, which further supports a lower ϕ value in the films than that in DCB/BN solutions.

On the assumption that $\phi = 0.83\%$ is the maximum value of ϕ, the lowest limit of hole mobility in PBPS is calculated to be $\Sigma\mu = 1.7 \times 10^{-2}$ cm^2/(V s), based on the above value of $\phi\Sigma\mu$ at the zero limit of C_{60} concentration ($\phi\Sigma\mu = 1.4 \times 10^{-4}$ cm^2/(V s)). Hoshino et al.[17] have reported a hole drift mobility of 1.35×10^{-4} cm^2/(V s) under an applied electric field of 4.9×10^5 V/cm for the PBPS polymer at room temperature using the conventional DC-TOF technique. The present TRMC technique probes the conductivity of the materials at a very low external electric field strength of ∼10^2 V/cm, induced by microwaves, while the direction of the electric field oscillates at 9.1 GHz. This is often called the AC technique.[21−24] The motion of charge carriers on extended conjugated segments in the polymer backbone contributes predominantly to the TRMC signals, leading to only small effects due to intersite hopping, trapping of charge carriers, etc. For this reason, the mobility observed in the present study is at least 2 orders of magnitude higher than that measured by the DC-TOF technique. Thus, the mobility of holes on a PBPS single chain is potentially over 1.7×10^{-2} cm^2/(V s) for PBPS fabricated free from impurities, defects, etc.

Conclusions

FP-TRMC measurements were successfully performed on PBPS film samples molecularly doped with electron acceptors. C_{60} was found to be a suitable dopant for PBPS. C_{60} does not contribute in the higher photon energy region (≥6.39 eV), and the high $\phi\Sigma\mu$ value (4.5×10^{-3} cm^2/(V s)) under excitation by 193-nm light can be attributed to the contribution of charge carriers that are produced due to direct ionization of the PBPS molecule. The generation of radical cations of PBPS at 406 nm due to the electron-transfer reaction between PBPS and C_{60} was investigated by laser flash photolysis with exposure by 532-nm light. An estimation of [PBPS$^{\bullet+}$] as 1.1×10^{-6} M^{-1} and the photocarrier generation yield ϕ as 0.83%, based on an absorbed photon density of 7.9×10^{16} cm^{-3}, gives a lowest limit of hole mobility in PBPS of 1.7×10^{-2} cm^2/(V s). The observed hole mobility of 1.7×10^{-2} cm^2/(V s) is 2 orders of magnitude higher than the mobility observed by the DC-TOF technique, 1.35×10^{-4} cm^2/(V s), in which the mobility of charge carriers is affected by intersite hopping, trapping of charge carriers, etc.

These results show that the high charge carrier mobility of PBPS polymer makes it a potential material for use in optoelectronic devices.

Acknowledgment. A. Acharya is grateful to the Japan Society for the Promotion of Science (JSPS) for providing financial assistance. The work was supported by a Grant-in-Aid from JSPS, Japan.

References and Notes

(1) Yuan, C. H.; Hoshino, S.; Toyoda, S.; Suzuki, H.; Fujiki, M.; Matsumoto, N. *Appl. Phys. Lett.* **1997**, *71*, 3326.

(2) Suzuki, H.; Hoshino, S.; Yuan, C. H.; Fujiki, M.; Toyoda, S.; Matsumoto, N. *IEEE J. Sel. Top. Quantum Electron.* **1998**, *4*, 129.

(3) Suzuki, H.; Hoshino, S.; Yuan, C. H.; Fujiki, M.; Toyoda, S.; Matsumoto, N. *Thin Solid Films* **1998**, *331*, 64.

(4) Hoshino, S.; Ebata, K.; Furukawa, K. *J. Appl. Phys.* **2000**, *87* (4), 1968.

(5) Hoshino, S.; Furukawa, K.; Ebata, K.; Breyl, I.; Suzuki, H. *J. Appl. Phys.* **2000**, *88* (6), 3408.

(6) Fujii, A.; Yoshimoto, K. *Jpn. J. Appl. Phys., Part 1* **1996**, *35*, 3914.

(7) Hattori, R.; Sugano, T.; Shirafuji, J.; Fujiki, T. *Jpn. J. Appl. Phys., Part 2* **1996**, *35*, L 1509.

(8) Suzuki, H. *Mol. Cryst. Liq. Cryst*. **1997**, *294*, 127.
(9) Suzuki, H. *J. Lumin.* **1997**,*72-74*, 1015.
(10) Hoshino, S.; Suzuki, H.; Fujiki, M.; Morita, M.; Matsumoto, N. *Synth. Met.* **1997**, *89*, 221.
(11) Xu, Y.; Fujino, T.; Naito, H.; Oka, K.; Dohmaru, T. *Chem. Lett*. **1998**, 229.
(12) Suzuki, H.; Hoshino, S.; Furukawa, K.; Ebata, K.; Yuan, C. H.; Bleyl, I. *Polym. Adv. Technol*. **2000**, *11*, 460.
(13) Sharma, A.; Lourderaj, U.; Deepak; Sathyamurthy, N.; Katiyar, M. *Comput. Mater. Sci*. **2005**, *33*, 206.
(14) Bleyl, I.; Ebata, K.; Hoshino, S.; Furukawa, K.; Suzuki, H. *Synth. Met.* **1999**, *105*, 17.
(15) Miller, R. D.; Michl, J. *Chem. Rev.* **1989**, *89*, 1359.
(16) Seki, S.; Matsui, Y.; Yoshida, Y.; Tagawa, S.; Koe, J. R.; Fujiki, M. *J. Phys. Chem. B* **2002**, *106*, 6849.
(17) Hoshino, S.; Furukawa, K.; Ebata, K.; Yuan, C. H.; Suzuki, H. *J. Appl. Phys*. **2000**, *88* (5), 2892.
(18) Furukawa, K.; Yuan, C. H.; Hoshino, S.; Suzuki, H.; Matsumoto, N. *Mol. Cryst. Liq. Cryst*. **1999**, *327*, 181.
(19) Scott, C. *Phys. World* **1998**, *11*, 21.
(20) Sirringhaus, H.; Wilson, R. J.; Friend, R. H.; Inabasekaran, M.; Wu, W.; Woo, E. P.; Grell, M.; Bradley, D. C. *Appl. Phys. Lett*. **2000**, 77 (3), 406.
(21) Hass, M. P.de; Warman, J. M. *Chem. Phys*. **1982**, *73*, 35.
(22) Savenije, T. J.; Hass, M. P.de; Warman, J. M. Z. *Phys. Chem.* **1999**, *212*, 201.
(23) Warman, J. M.; Gelinck, G. H.; Hass, M. P.de. *Condens. Matter* **2002**, *14*, 9935.
(24) Grozema, F. C.; Siebbeles, L. D. A.; Warman, J. M.; Seki, S.; Tagawa, S.; Scherf, U. *Adv. Mater.* **2002**, *14*, 228.
(25) Kroeze, J. E.; Savenije, T. J.; Vermeulene, M. J. W.; Warman, J. M. *J. Phys. Chem. B* **2003**, *107*, 7696.
(26) Acharya, A.; Seki, S.; Saeki, A.; Koizumi, Y.; Tagawa, S. *Chem. Phys. Lett*. **2005**, *404* (4−6), 356.
(27) Saeki, A.; Seki, S.; Koizumi, Y.; Sunagawa, T.; Kiminori, U.; Tagawa, S. *J. Phys. Chem. B* **2005**, *109* (20), 10015.
(28) Kepler, R. G.; Cahill, P. A. *Appl. Phys. Lett*. **1993**, *63*, 1552.
(29) Nakayama, Y.; Saito, A.; Fujii, T.; Akita, S. J. *Imaging Sci. Technol*. **1999**, *43*, 261.
(30) Wang, K. A. *Nature* **1992**, *356*, 585.
(31) Nešpůrek, S.; Wang, G.; Böhm, S.; Kořinek, M.; Adler, H. J. *Macromol. Symp*. **2004**, *210*, 513.
(32) Seki, S.; Yoshida, Y.; Tagawa, S.; Asai, K. *Macromolecules* **1999**, *32*, 1080.
(33) Seki, S.; Koizumi, Y.; Kawaguchi, T.; Habara, H.; Tagawa, S. *J. Am. Chem. Soc.* **2004**, *126*, 3521.
(34) Koe, J. R.; Fujiki, M.; Nakashima, H. *J. Am. Chem. Soc.*, **1999**, *121*, 9734.
(35) Nakashima, H.; Fujiki, M.; Koe, J. R. *Macromolecules* **1999**, *32*, 7707.
(36) Yoshino, K.; Yin, H. X.; Morita, S.; Kawai, T.; Zakhidov, A. A. *Solid State Commun*. **1993**, *85*, 85.
(37) Watanabe, A.; Ito, O. *J. Phys. Chem*. **1994**, *98*, 7736.
(38) Savenije, T. J.; Kroeze, J. E.; Wienk, M. M.; Kroon, J. M.; Warman, J. M. *Phys. Rev.* **2004**, *B 69*, 155205.
(39) Acharya, A.; Seki, S.; Saeki, A.; Tagawa, S. *Solid State Commun*., submitted for publication, 2005.
(40) Van Walree, C. A.; Cleiki, T. J.; Jenneskens, L. W.; Vlietstra, E. J.; Van der Laan, G. P.; De Hass, M. P.; Lutz, E. G. *Macromolecules* **1996**, *29*, 7362.
(41) Seki, S.; Yoshida, Y.; Tagawa, S.; Asai, K.; Ishigure, K.; Furukawa, K.; Fujiki, M.; Matsumoto, N. *Philos. Mag. B* **1999**, *79*, 1631.
(42) Matsui, Y. Nishida, K.; Seki, S.; Yoshida, Y.; Tagawa, S.; Yamada, K.; Imahori, H.; Sakata, Y. *Organometallics* **2002**, *21*, 5144.
(43) Matsui, Y.; Seki, S.; Tagawa, S. *Chem. Phys. Lett*. **2002**, *357*, 346.
(44) Seki, S.; Terashima, Y.; Kunimi, Y.; Kawamori, T.; Tashiro, M.; Honda, Y.; Tagawa, S. *RPC*, **2003**, *68*, 501.
(45) Kawaguchi, T.; Seki, S.; Okamoto, K.; Saeki, A.; Yoshida, Y.; Tagawa, S. *Chem. Phys. Lett*. **2003**, *374*, 353.
(46) Yong, Y.; Man, Z. Z.; Xi, P. X.; Qi, H. H. *Spectrosc. lett*. **1999**, *32*, 535.